



Published in final edited form as:

Cancer Discov. 2015 March ; 5(3): 264–273. doi:10.1158/2159-8290.CD-14-0293.

Ligand independent EphA2 signaling drives the adoption of a targeted therapy-mediated metastatic melanoma phenotype

Kim H. T. Paraiso¹, Meghna Das Thakur², Bin Fang³, John M. Koomen¹, Inna V. Fedorenko⁴, Jobin K. John¹, Hensin Tsao⁵, Keith T. Flaherty⁶, Vernon K. Sondak⁷, Jane L. Messina^{7,8}, Elena B. Pasquale⁹, Alejandro Villagra¹⁰, Uma N. Rao¹¹, John M. Kirkwood¹¹, Friedegund Meier¹², Sarah Sloat⁷, Geoffrey T. Gibney⁷, Darrin Stuart², Hussein Tawbi¹¹, and Keiran S.M. Smalley^{4,6,*}

¹The Department of Molecular Oncology, Moffitt Cancer Center & Research Institute, 12902 Magnolia Drive, Tampa, FL, 33612

²Novartis Institute for Biomedical Research, Emeryville, CA

³The Proteomics Core, Moffitt Cancer Center & Research Institute, 12902 Magnolia Drive, Tampa, FL, 33612

⁴The Department of Tumor Biology, Moffitt Cancer Center & Research Institute, 12902 Magnolia Drive, Tampa, FL, 33612

⁵Department of Surgery, Massachusetts General Hospital, Boston, MA

⁶Department of Medicine, Massachusetts General Hospital, Boston, MA

⁷The Department of Cutaneous Oncology, Moffitt Cancer Center & Research Institute, 12902 Magnolia Drive, Tampa, FL, 33612

⁸The Department of Anatomic Pathology, Moffitt Cancer Center & Research Institute, 12902 Magnolia Drive, Tampa, FL, 33612

⁹Sanford-Burnham Medical Research Institute, La Jolla, CA

¹⁰The Department of Immunology, Moffitt Cancer Center & Research Institute, 12902 Magnolia Drive, Tampa, FL, 33612

¹¹Division of Hematology/Oncology, Department of Medicine, School of Medicine, University of Pittsburgh, University of Pittsburgh Cancer Institute, Pittsburgh, PA

¹²Department of Dermato-Oncology, University of Tuebingen, Tuebingen, Germany

Abstract

Many patients with BRAF inhibitor resistance can develop disease at new sites, suggesting that drug-induced selection pressure drives metastasis. Here we used mass spectrometry-based phosphoproteomic screening to uncover ligand-independent EphA2 signaling as an adaptation to

*To whom correspondence should be addressed. The Moffitt Cancer Center & Research Institute, Department of Molecular Oncology, 12902 Magnolia Drive, Tampa, FL, 33612, USA. Tel: 813-745-8725 Fax: 813-449-8260, keiran.smalley@moffitt.org.

The authors declare no conflict of interest

BRAF inhibitor therapy that led to the adoption of a metastatic phenotype. The EphA2-mediated invasion was AKT-dependent and readily reversible upon removal of drug as well as through PI3K and AKT inhibition. In xenograft models, BRAF inhibition led to the development of EphA2 positive metastases. A retrospective analysis of melanoma patients on BRAF inhibitor therapy showed that 68% of those failing therapy develop metastases at new disease sites, compared to 35% in patients on dacarbazine. Further IHC staining of melanoma specimens taken from patients on BRAF inhibitor therapy as well as metastatic samples taken from patients failing therapy showed increased EphA2 staining. We suggest that inhibition of ligand-independent EphA2 signaling may limit metastases associated with BRAF inhibitor therapy.

Introduction

Acquired resistance is the major factor that limits the long-term efficacy of targeted therapy in melanoma patients (1). The patterns of disease recurrence seen at progression are complex, with 50% of individuals progressing at sites of new metastasis only, 44% at existing sites of metastasis and 6% at both existing and new sites (2). A number of putative escape mechanisms to BRAF inhibitors have now been described, with the recovery of mitogen-activated protein kinase (MAPK) signaling known to occur in >70% of lesions that progress on therapy (1). The continued MAPK dependency of BRAF inhibitor resistant melanomas led to the initiation of clinical trials to evaluate the BRAF/MEK inhibitor combination (3). Despite BRAF/MEK inhibition showing improved progression-free survival compared to BRAF inhibitor alone, resistance was still widespread (3). To date, most of the clinically validated mechanisms of BRAF and BRAF/MEK inhibitor resistance are genetic and include acquired mutations that reactivate the MAPK pathway (*BRAF* splice mutants, *NRAS* mutations, *MEK1/2* mutations) as well as genetic changes that increase PI3K/AKT signaling (*NF1*, *PTEN*, *PI3KCA* and *AKT1*) (4–9). It has also been shown that increased receptor tyrosine kinase (RTK) signaling, secondary to the relief of feedback inhibition in the MAPK pathway, facilitates escape from BRAF and MEK inhibition (10, 11). There is evidence from other tumor histologies that therapeutic intervention drives the adoption of phenotypes such as an epithelial-to-mesenchymal transition (EMT) (12). Although it is known that melanoma cells with intrinsic BRAF inhibitor resistance frequently show increased invasive potential, the role of chronic BRAF inhibitor treatment in mediating the dissemination of melanoma cells has been little explored (13).

Ephrins constitute the largest family of RTKs and play diverse roles in cell migration, development and maintenance of the stem cell niche (14, 15). Under physiological conditions, EphA2 kinase binds to its membrane bound ligand Ephrin A1, leading to the inhibition of AKT and reduced cell migration (14). In cancer, EphA2 is often overexpressed and, following phosphorylation by AKT at S897, can signal in a ligand-independent manner to drive tumorigenic behavior and increased cell migration (16, 17). In the present study we utilized a label-free phosphoproteomic approach to quantify all of the phosphorylation events associated with long-term inhibition of BRAF signaling. These analyses revealed a previously unsuspected link between BRAF and BRAF/MEK inhibition and the adoption of an aggressive, invasive phenotype driven through ligand-independent EphA2 signaling.

Results

Phosphoproteomics identifies BRAF inhibitor resistance to be associated with an invasive signature

We began by asking how chronic vemurafenib treatment rewired the signaling network of *BRAF* mutant melanoma at a systems level through the use of a mass spectrometry-based phosphoproteomic platform. The goal of these studies was to uncover phenotypic adaptations to chronic BRAF inhibition. Our approach offers advantages over other proteomic methods such as reverse phase protein array (RPPA) in being comprehensive, unbiased and not limited by antibody availability. In brief, tyrosine phosphorylated peptides were retrieved by immunoprecipitation and the threonine and serine phosphorylated peptides isolated by subjecting the resulting flow-through to strong cation exchange (SCX) and immobilized metal affinity chromatography (IMAC). Liquid chromatography tandem mass spectrometry (LC-MS/MS) was used to quantify all of the phospho-peptides from isogenic vemurafenib naïve and resistant 1205Lu melanoma cells. Levels of peptide phosphorylation were quantified using MaxQuant and the protein-protein interactions characterized using GeneGO (18, 19). Cytoscape mapping of the global signaling changes showed an increase in both the number of nodes and the number of edges in vemurafenib resistant 1205Lu cells (Naïve: 544 nodes, 1208 edges. Resistant: 552 nodes, 1288 edges). Chronic BRAF inhibition was associated with an enrichment of phospho-proteins involved in adhesion, cytoskeletal remodeling, FAK and integrin signaling (Figure 1A) as well as the emergence of a highly interconnected resistance interactome involving EphA2, EGFR, EphB4, FAK1, HDAC1, integrins (ITGA3, ITGA5, ITGAV, ITGB1, ITGB5), nucleolin, p130CAS, paxillin, SHC1, Tensin-3 and Zyxin (Figures 1B,C). As this suggested the adoption of a migratory/invasive phenotype, we next characterized a panel of BRAF (designated “R” cell lines) and BRAF/MEK inhibitor resistant cell lines (designated “RR”), which were generated through chronic drug treatment for >6 months (Supplemental Figure 1). It was noted that the resistant cell lines had increased motile behavior in both transendothelial migration assays (where melanoma cells were allowed to migrate through confluent endothelial cell monolayers), and 3D spheroid assays (in which melanoma cells migrated into the surrounding collagen matrix) (Figure 1D, Supplemental Figure 2, and not shown). One potential candidate identified from the screen was EphA2, a cell surface receptor tyrosine kinase implicated in development, stem cell niche maintenance and cancer progression (14).

Ligand-independent EphA2 signaling drives the adoption of an invasive phenotype

Despite EphA2 being implicated in the suppression of cell adhesion and migration following stimulation with ephrin-A1, it can also function in a forward signaling, ligand-independent manner following phosphorylation by AKT at S897 (16) (See Model in Supplemental Figure 3). Validation of the phosphoproteomic screen through Western blotting showed increased EphA2, phospho-EphA2 (S897), phospho-FAK (Y397), phospho-Paxillin (Y118) and total Paxillin expression in BRAF inhibitor resistant cell lines (Figure 2A). Increased S897-EphA2 expression was also observed in other BRAF inhibitor resistant (R) cell lines as well as those with acquired BRAF/MEK inhibitor resistance (RR) (Figure 2B). An analysis of drug-naïve 1205Lu and A375 melanoma cells (which expressed low-levels of EphA2

basally) did not reveal vemurafenib to increase EphA2 phosphorylation at S897, - with the addition of drug instead reducing phosphorylation at this site (Supplemental Figure 4). This, along with two previous studies showing that vemurafenib and its analogue PLX4720 did not alter EphA2 kinase activity in *in vitro* assays, suggested that the induction of ligand-independent EphA2 signaling was not a direct consequence of BRAF inhibitor treatment (20, 21). In epithelial cancers, unrestricted forward EphA signaling is accompanied by decreased ephrin ligand expression (16). The loss of bidirectional Ephrin-Eph signaling in cell lines with acquired BRAF and BRAF/MEK inhibitor resistance was suggested by the reduction of ephrin-A1 ligand expression (Figure 2C) and the ability of exogenous ephrin-A1 ligand to suppress the invasion of vemurafenib resistant 1205LuR cells in a matrigel assay, in which cells migrated towards serum (Figure 2D). In drug resistant melanoma cells, siRNA knockdown of EphA2 led to a significant ($P < 0.005$) abrogation of invasiveness in a matrigel invasion assay in both the presence and absence of drug, but did not resensitize the cells to vemurafenib-mediated apoptosis (3 μ M, 48 hrs) (Figures 2E,F and Supplemental Figures 5,6). Conversely, the introduction of EphA2 into a melanoma cell line that lacked its expression increased cell invasion through matrigel (Figure 2G). To rule out that the inhibition of invasion was due to cell death, we also performed Annexin V/DAPI staining and found no differences between non-targeting and EphA2 siRNA treated cohorts (data not shown).

Ligand-independent EphA2 signaling is AKT-dependent

In all cases, S897 phosphorylation of EphA2 was mediated through PI3K/AKT, with Western blotting showing the resistance phenotype to be associated with increased phospho-AKT and phospho-GSK3 β levels (Figure 3A and Supplemental Figure 7A) and the ability of a PI3K (GDC-0941, 3 μ M) and an AKT inhibitor (MK-2206, 3 μ M) to reverse receptor phosphorylation (Figure 3B). Further studies showed PI3K inhibition (PI-103, 1 μ M) to prevent melanoma cell invasion in a 3D spheroid assay (Figure 3C). Treatment with the ephrin-A1 ligand restored EphA2 tyrosine phosphorylation (Y772), and thus kinase activity, inhibited AKT phosphorylation on S473, AKT-dependent EphA2 phosphorylation at S897 and FAK phosphorylation at Y397 (Figure 3D and Supplemental Figures 7B,C). The potential role of FAK signaling in the drug-mediated invasive phenotype was suggested by the ability of the FAK inhibitor PF-228 to inhibit invasion in a 3D spheroid assay (Supplemental Figure 7C). Introduction of an EphA2 S897A mutant that is refractory to AKT-mediated phosphorylation prevented its interaction with an AKT substrate (Figure 3E) and reversed the invasion of BRAF inhibitor resistant cells through matrigel and their migration in a scratch assay (Figure 3F). Although increased phosphorylation by AKT explained the ligand-independent EphA2 signaling, it did not explain the increased EphA2 expression in BRAF inhibitor-resistant melanoma cells. We therefore asked whether EphA2 expression in BRAF inhibitor resistant cell lines was dependent upon continuous drug selection pressure. Removal of BRAF or BRAF/MEK inhibition led to an initial decrease in the fitness of the resistant cells as seen by an increased doubling time, followed by the partial reversal of resistance (Supplemental Figures 8–9) - an effect associated with decreased phosphorylation of both AKT and EphA2 S897 (Supplemental Figure 10A). Phenotypically, these effects were paralleled by a marked reduction in the invasive capacity of the cells (Supplemental Figures 10B,C).

Ligand-independent EphA2 signaling is induced *in vivo* following BRAF inhibition and is associated with metastatic dissemination

The *in vivo* relevance of ligand-independent EphA2 signaling and its link to metastasis was explored in melanoma patient specimens. It was found that whereas 0% of primary (stage I/II) melanoma lesions (n=12) stained strongly (+2/3) for EphA2, 21% of metastatic lesions (stage III/IV) (n=19) showed strong staining (Figure 4A,B: Supplemental Table 1), with 57.9% of metastatic lesions showing some strong focal S897-EphA2 staining. We next established an *in vivo* resistance model where fragments of treatment naïve human melanoma specimens were implanted subcutaneously into nude mice (patient-derived xenografts, PDX) (22). Vemurafenib dosing was commenced over 100–200 days, until resistance emerged (22). Local or distant metastases were frequently observed in vemurafenib resistant PDXs, but not in the vehicle treated animals (as these were sacrificed at much earlier time points). Staining of matched pairs of subcutaneous and metastatic specimens from the same drug-treated animals at necropsy showed high levels of immunohistochemical staining for EphA2 in the metastatic lesions that were absent from the matched primary subcutaneous lesions (Figure 4C). In common with other studies, a heterogeneous pattern of EphA2 staining was noted, with both membranous and cytoplasmic/nuclear staining observed (17).

Analysis of specimens from a cohort of 6 melanoma patients receiving vemurafenib therapy (14–370 days) revealed increased EphA2 and S897-EphA2 expression in the majority of on-treatment and post-relapse samples that were lacking in the pre-treatment lesions (5/6) (Supplemental Table 2: Figure 4D shows pre and post treatment specimens from patient E). Chronic treatment of A375 cells with vemurafenib (1 μ M, 1–4 weeks) further supported the rapid induction of EphA2 and S897-EphA2 expression following BRAF inhibition, with increased EphA2 protein expression observed by 3 weeks and increased EphA2 and S897-EphA2 expression seen after 4 weeks of drug treatment (Supplemental Figure 11). It thus seemed that induction of EphA2 expression was a relatively rapid adaptation to BRAF inhibition, which may precede the development of acquired drug resistance.

A potential link between acquired resistance and the role of BRAF inhibition in the emergence of new metastases was suggested by the observation patients failing vemurafenib therapy (n=28) had significantly higher incidence of tumor growth at new, distant disease sites (68%) rather than the regrowth of existing lesions, compared to patients receiving dacarbazine (n=20) (35%) (Supplemental Table 3). These differences were seen despite the time on therapy being similar (147.5 days vs 101.5 days for vemurafenib and dacarbazine, respectively, p=0.1379) (Supplemental Table 3). We next determined whether EphA2 expression increased in new metastatic lesions that arose on BRAF inhibitor therapy. The IHC staining of a pair of matched pre-treatment and therapy-derived metastases from a patient failing vemurafenib therapy showed high levels of EphA2, phospho-EphA2 and phospho-AKT expression in the treatment-derived metastatic lesions (Figure 4E), with much less EphA2 expression observed in the pre-treatment primary lesion.

Discussion

Hostile microenvironments such as hypoxia, metabolic changes and nutrient deprivation favor the detachment of cancer cells and their migration to more favorable niches (23, 24). We here demonstrate that chronic BRAF inhibition induces a migratory, invasive phenotype in melanoma cells. In epithelial tumors, therapeutic adaptation leads to an EMT, which is sometimes associated with increased tumor invasiveness and metastatic spread (12, 25). Phosphoproteomic screening identified ligand-independent EphA2 signaling as a key driver of the metastatic phenotype in melanoma cells with acquired BRAF and BRAF/MEK inhibitor resistance. In agreement with this, increased S897 phosphorylated EphA2 was identified in on-treatment melanoma metastases. Our findings mirror those in astrocytoma, where tumor aggressiveness was correlated with high expression of S897 phosphorylated EphA2 as well as phospho-AKT (16). In prostate cancer and glioma cell lines, ligand-independent EphA2 signaling is known to promote invasion in an AKT-dependent manner and was reversed following treatment with Ephrin-A1 ligand (16).

Previous modeling studies have demonstrated BRAF inhibitor resistance to be dependent upon continuous drug administration, with treatment withdrawal leading to tumor regression (22). It was further observed that ligand-independent EphA2-mediated invasion also required constant BRAF and BRAF/MEK inhibitor-mediated selection pressure. The reversibility of the invasive phenotype upon drug removal suggested that ligand-independent EphA2 signaling could be abrogated through alternate dosing schedules. There is currently some debate as to whether intermittent BRAF/MEK inhibitor dosing can forestall resistance better than continuous dosing, with evidence being provided for each scenario (22, 26). There is also clinical evidence that continuation of drug beyond the time of progression can prolong clinical benefit (22, 26). Our data support the notion that continuous drug dosing can increase the fitness and the metastatic potential of the melanoma cells. It is likely that this could be overcome through intermittent drug dosing and this may limit the development of new metastases.

Therapeutically, tyrosine kinase inhibitors directed against EphA2 are unlikely to reverse the migration driven through the EphA2/AKT axis. Instead, direct targeting of the EphA2 receptor with agonists should inhibit both ligand-independent EphA2 signaling and AKT signaling, limiting metastatic dissemination. Targeting of EphA2 could be an excellent strategy to increase response duration by limiting the development of new disease in patients on BRAF and BRAF/MEK inhibitor therapies.

Materials and Methods

Cell culture and generation of BRAF inhibitor resistance

Cells were cultured in 5% FBS, RPMI 1640 media. Parental 1205Lu, SK-MEL-28, and WM164 melanoma cells lines were a gift from Dr. Meenhard Herlyn (The Wistar Institute, Philadelphia, PA). Parental A375 cell line was purchased from American Type Culture Collection on April 18th 2012. Identities of all cell lines were confirmed by Biosynthesis Inc., through short tandem repeat validation analysis at 6 monthly intervals. The date of last validation for these studies was December 20th 2013. Dual BRAF and MEK inhibitor

resistant (RR) lines were established by chronically treating 1205Lu, SK-MEL-28, and WM164 for >6 months with 1 μ M each vemurafenib and selumetinib. Unless otherwise noted, single-agent vemurafenib (R) cell lines were maintained in 5% media with the addition of vemurafenib at the following concentrations: 1 μ M for A375R, 2 μ M for WM164R, and 3 μ M for 1205LuR. Dual agent RR inhibitor resistant lines were maintained in 5% FBS, RPMI 1640 with 1 μ M vemurafenib and 1 μ M selumetinib.

Proliferation assay

Assays were performed as described in (27). Briefly, 4,000 cells were seeded into each well of a 96-well plate prior to drug treatment and allowed to attach overnight. Media containing inhibitor solubilized in DMSO, or an equivalent volume of DMSO alone was added and cells incubated for 3 days prior to the addition of Alamar blue reagent (Invitrogen, Carlsbad, CA).

Inhibitors

Vemurafenib (PLX4032), selumetinib (AZD6244), GDC-0941, LBH589, PI-103 and MK-2206 were purchased from Selleck Chemicals (Houston, TX, USA). Dabrafenib and trametinib were from Chemie Tek (Indianapolis, IN, USA).

Phosphoproteomic analysis: Sample Processing

Naïve and vemurafenib resistant 1205Lu cell lines were each grown in ten 15 cm tissue culture dishes. Cells were grown to ~70% confluency prior to washing each dish with 10ml of ice cold PBS + 1mM orthovanadate (Sigma Aldrich, St. Louis, MO). Cells were then lysed according to the manufacturer's instructions for the Phospho-Tyrosine Mouse mAb (P-Tyr-100) (Cell Signaling, Beverly, MA). Lysed proteins were reduced and alkylated prior to proteolytic digestion and phosphorylated tyrosine containing peptides generated from tryptic digestion were enriched with antibody-based (P-Tyr-100) immunoprecipitation. Flow through from the immunoprecipitation was then further enriched for phosphorylated serines and threonines by strong cation exchange peptide fractionation (SCX) and immobilized metal affinity chromatography (IMAC). The enriched phospho tyrosine, serine and threonine fractions were then subjected to liquid chromatography tandem mass spectrometry (LC-MS/MS) and the resultant tandem mass spectra was searched against SEQUEST and MASCOT databases to identify phosphoproteins. To calculate relative phospho-signal intensities, label-free protein quantification of the mass spectrometry data was analyzed using MaxQuant version 1.2.2.5 (18).

EphA2 and S897A mutant plasmid transfection

The human EphA2 plasmid was generated as described in (28). The mutant S897A plasmid was a gift from Dr. Elena Pasquale. Naïve SK-MEL-28 cells were transfected with 4 μ g of EphA2 or control plasmid while 1205LuR cells were transfected with 4 μ g of S897A or WT EphA2 control plasmid with Lipofectamine (Invitrogen, Carlsbad, CA, USA) according to the manufacturer's instructions. Stable transfectants were harvested at 14 days and protein expression levels were confirmed by Western blotting.

Western blotting

Proteins were extracted and blotted as described in (27). Antibodies against S897-EphA2, Y772-EphA2, EphA2, Y397-FAK, FAK, Y118-PXN, PXN, S9-GSK3, GSK3 β , S473-AKT, AKT, phospho-S/T AKT substrate and PTEN were purchased from Cell Signaling Technology (Danvers, MA). Anti-ephrinA1 was from Santa Cruz Biotechnology (Santa Cruz, CA) while GAPDH was purchased from Sigma Aldrich.

RNA interference

Cells were transfected as described in (27) with 25nmol/L EphA2 and scrambled siRNA sequences (LifeTechnologies, Carlsbad, CA). Cells were transfected for 24 hours in the absence of inhibitor and an additional 48 hours in the presence of inhibitor prior to further experimentation.

Quantitative real-time PCR

Q-RT-PCR was performed as described in (27). TaqMan Gene Expression Assay Hs00171656_m1 primers/probe were used to quantify EphA2. The 18S (P/N 4319413E) and GAPDH (Hs99999905_m1) used to normalize EphA2. All standards and samples were tested in triplicate and data were analyzed using SDS software version 2.3.

3D spheroid assays

Collagen implanted spheroids were prepared using the liquid overlay method as described in (27) and were treated with 100 nM LBH589 or 1 μ M PI-103 for 120 hours before being analyzed by fluorescence microscopy. Calculations of the areas of spheroid invasion into the collagen matrix were performed with ImageJ analysis software.

Transendothelial cell migration assays

Migration assays were performed as described in (29). Human umbilical vein endothelial cells (HUVECs) were plated into transwell inserts and grown to confluence. DiI labeled naïve or resistant melanoma cell lines were plated on top of the HUVEC layer and allowed to invade for 1–4 hours. Non-migratory cells were removed prior to imaging with an inverted Nikon Eclipse TS100 microscope. Calculations of the percent spheroid invasion into the collagen matrix were performed with ImageJ analysis software.

Scratch wound assays

S897A and control plasmid transfected 1205LuR melanoma were grown to confluency prior to scratching with a p20 pipette tip. Wounds were imaged at 0 and 24 hours and percentage wound closure was calculated using ImageJ software 1.46r.

Matrigel invasion assays

Cells were overlaid onto transwell inserts coated with Matrigel (BD) and allowed to invade for 24–48 hours. For ephrin A1 ligand experiments, cells were pretreated for 72 hours with 1 μ g/mL ephrinA1-Fc or IgG-Fc ((R&D Systems). Cells were fixed and stained with phalloidin-AF594 and non-invasive cells removed prior to fluorescence imaging with an inverted Nikon Eclipse TS100 microscope. To quantify levels of invasion, fixed and stained

cells were imaged with a Zeiss confocal microscope (20x) at 0 μm with 0.5 μm image slices taken throughout the distance of invasion.

Rates of new metastasis for vemurafenib and dabrafenib treated patients

Patients managed at the Moffitt Cancer Center were selected from Moffitt medical records and archived melanoma specimens under the TCC/HRI and Moffitt pathology systems with written informed consent being approved by the Institutional Review Board of the University of South Florida under the Declaration of Helsinki Protocols. For the vemurafenib and dabrafenib treated patients, the target population consisted of subjects with unresectable stage III or stage IV *BRAF* V600E mutant cutaneous melanoma treated with single-agent vemurafenib or dabrafenib as the first line of therapy. A similar patient cohort was also identified who received dacarbazine as their first line of therapy. Patients were selected for each treatment regimen who had similar numbers of restaging scans to eliminate sample bias. De-identified information pertaining to patient demographics and clinical outcome during therapy was collected on subjects with exclusion of patients who completed less than 2 months of therapy or for whom follow-up information was not available.

Xenograft studies

Xenograft implantation of tumor pieces from the subcutaneous tissue of a vemurafenib treatment naïve 44 year-old male with recurrent *BRAF* V600E mutant melanoma (HMEX2613) was performed as described in (22) under an approved Novartis IACUC protocol. Established HMEX2613 tumors were dosed continuously with 45mg/kg vemurafenib. After 100–200 days, tumors became resistant to vemurafenib with 30% of mice being euthanized due to clinical signs. Upon necropsy, widespread metastasis was found. IHC was carried out on subcutaneous resistant tumors and matched with corresponding metastatic lesions.

Immunohistochemistry: Xenograft and patient samples

Slides were stained using the Ventana Discovery XT automated system (Ventana Medical Systems, Tucson, AZ) per manufacturer's instructions with proprietary reagents. Slides were deparaffinized on the automated system with EZ Prep solution (Ventana). The retrieval method used was citrate buffer at pH 6.0. Rabbit anti-mouse polyclonal IgG primary antibody for EphA2 (Santa Cruz Biotechnology, Santa Cruz, CA, #sc-924) that reacts to human EphA2 was used at a 1:250 concentration in PSS antibody diluent (Ventana) and incubated for 12 min. Ventana Anti-mouse secondary antibody was used for 12 min and Ventana OmniMap kit used for detection. Slides were counterstained with Hematoxylin. De-identified formalin-fixed paraffin-embedded tissue samples were obtained from the Moffitt Pathology, the University of Pittsburgh and the University of Tuebingen archives under a written informed consent protocol approved by the Institutional Review Board of the University of South Florida under the Declaration of Helsinki Protocols and stained as above for the xenograft samples. Staining was visualized using the Ventana Chromomap Redkit. Slides were analyzed by two independent observers and consensus scored on a scale from (0 to +3).

Statistical analysis

Data show the mean of at least 3 independent experiments \pm the SE mean, unless stated otherwise. GraphPad Prism 6 statistical software were used to perform the 2-tailed Student's *t*-test and for contingency analyses of patient data (2-tailed Fisher's exact test). For all statistical analyses, asterisks (*) indicates $P < 0.05$.

Supplementary Material

Refer to Web version on PubMed Central for supplementary material.

Acknowledgments

Grant support: Work in the Smalley lab is supported by R01 CA161107-01 and SPORE grant P50 CA168536-01A1 from the National Institutes of Health. Sarah Sloat received a grant from the Melanoma and Sarcoma Groningen Foundation. Inna Fedorenko was supported by the Joanna M. Nicolay Melanoma Foundation.

References

1. Chapman PB, Hauschild A, Robert C, Haanen JB, Ascierto P, Larkin J, et al. Improved survival with vemurafenib in melanoma with BRAF V600E mutation. *The New England journal of medicine*. 2011; 364:2507–16. [PubMed: 21639808]
2. Menzies AM, Haydu LE, Carlino MS, Azer MW, Carr PJ, Kefford RF, et al. Inter- and intra-patient heterogeneity of response and progression to targeted therapy in metastatic melanoma. *PLoS ONE*. 2014; 9:e85004. [PubMed: 24400126]
3. Flaherty KT, Infante JR, Daud A, Gonzalez R, Kefford RF, Sosman J, et al. Combined BRAF and MEK inhibition in melanoma with BRAF V600 mutations. *The New England journal of medicine*. 2012; 367:1694–703. [PubMed: 23020132]
4. Shi H, Hong A, Kong X, Koya RC, Song C, Moriceau G, et al. A Novel AKT1 Mutant Amplifies an Adaptive Melanoma Response to BRAF Inhibition. *Cancer Discov*. 2014; 4:69–79. [PubMed: 24265152]
5. Shi H, Hugo W, Kong X, Hong A, Koya RC, Moriceau G, et al. Acquired Resistance and Clonal Evolution in Melanoma during BRAF Inhibitor Therapy. *Cancer Discov*. 2014; 4:80–93. [PubMed: 24265155]
6. Poulidakos PI, Persaud Y, Janakiraman M, Kong X, Ng C, Moriceau G, et al. RAF inhibitor resistance is mediated by dimerization of aberrantly spliced BRAF(V600E). *Nature*. 2011; 480:387–90. [PubMed: 22113612]
7. Nazarian R, Shi H, Wang Q, Kong X, Koya RC, Lee H, et al. Melanomas acquire resistance to B-Raf(V600E) inhibition by Rtk or N-Ras upregulation. *Nature*. 2010; 468:973–7. [PubMed: 21107323]
8. Paraiso KH, Xiang Y, Rebecca VW, Abel EV, Chen YA, Munko AC, et al. PTEN loss confers BRAF inhibitor resistance to melanoma cells through the suppression of BIM expression. *Cancer Research*. 2011; 71:2750–60. [PubMed: 21317224]
9. Wagle N, Van Allen EM, Treacy DJ, Frederick DT, Cooper ZA, Taylor-Weiner A, et al. MAP Kinase Pathway Alterations in BRAF-Mutant Melanoma Patients with Acquired Resistance to Combined RAF/MEK Inhibition. *Cancer Discov*. 2014; 4:61–68. [PubMed: 24265154]
10. Abel EV, Basile KJ, Kugel CH 3rd, Witkiewicz AK, Le K, Amaravadi RK, et al. Melanoma adapts to RAF/MEK inhibitors through FOXD3-mediated upregulation of ERBB3. *The Journal of clinical investigation*. 2013; 123:2155–68. [PubMed: 23543055]
11. Lito P, Pratilas CA, Joseph EW, Tadi M, Halilovic E, Zubrowski M, et al. Relief of Profound Feedback Inhibition of Mitogenic Signaling by RAF Inhibitors Attenuates Their Activity in BRAFV600E Melanomas. *Cancer Cell*. 2012; 22:668–82. [PubMed: 23153539]

12. Yu M, Bardia A, Wittner BS, Stott SL, Smas ME, Ting DT, et al. Circulating breast tumor cells exhibit dynamic changes in epithelial and mesenchymal composition. *Science*. 2013; 339:580–4. [PubMed: 23372014]
13. O'Connell MP, Marchbank K, Webster MR, Valiga AA, Kaur A, Vultur A, et al. Hypoxia induces phenotypic plasticity and therapy resistance in melanoma via the tyrosine kinase receptors ROR1 and ROR2. *Cancer Discov*. 2013; 3:1378–93. [PubMed: 24104062]
14. Pasquale EB. Eph receptors and ephrins in cancer: bidirectional signalling and beyond. *Nature reviews Cancer*. 2010; 10:165–80.
15. Murai KK, Pasquale EB. Restraining stem cell niche plasticity: a new talent of Eph receptors. *Cell Stem Cell*. 2010; 7:647–8. [PubMed: 21112558]
16. Miao H, Li DQ, Mukherjee A, Guo H, Petty A, Cutter J, et al. EphA2 Mediates Ligand-Dependent Inhibition and Ligand-Independent Promotion of Cell Migration and Invasion via a Reciprocal Regulatory Loop with Akt. *Cancer Cell*. 2009; 16:9–20. [PubMed: 19573808]
17. Binda E, Visioli A, Giani F, Lamorte G, Copetti M, Pitter KL, et al. The EphA2 receptor drives self-renewal and tumorigenicity in stem-like tumor-propagating cells from human glioblastomas. *Cancer Cell*. 2012; 22:765–80. [PubMed: 23238013]
18. Cox J, Hein MY, Lubner CA, Paron I, Nagaraj N, Mann M. Accurate proteome-wide label-free quantification by delayed normalization and maximal peptide ratio extraction, termed MaxLFQ. *Mol Cell Proteomics*. 2014; 13:2513–26. [PubMed: 24942700]
19. Fedorenko IV, Fang B, Munko AC, Gibney GT, Koomen JM, Smalley KS. Phosphoproteomic analysis of basal and therapy-induced adaptive signaling networks in BRAF and NRAS mutant melanoma. *Proteomics*. 2014 Oct 22. Epub ahead of print. 10.1002/pmic.201400200
20. Bollag G, Hirth P, Tsai J, Zhang J, Ibrahim PN, Cho H, et al. Clinical efficacy of a RAF inhibitor needs broad target blockade in BRAF-mutant melanoma. *Nature*. 2010; 467:596–9. [PubMed: 20823850]
21. Davis MI, Hunt JP, Herrgard S, Ciceri P, Wodicka LM, Pallares G, et al. Comprehensive analysis of kinase inhibitor selectivity. *Nature Biotechnology*. 2011; 29:1046–51.
22. Das Thakur M, Salangsang F, Landman AS, Sellers WR, Pryer NK, Levesque MP, et al. Modelling vemurafenib resistance in melanoma reveals a strategy to forestall drug resistance. *Nature*. 2013; 494:251–5. [PubMed: 23302800]
23. Friedl P, Alexander S. Cancer invasion and the microenvironment: plasticity and reciprocity. *Cell*. 2011; 147:992–1009. [PubMed: 22118458]
24. Lee SL, Rouhi P, Dahl Jensen L, Zhang D, Ji H, Hauptmann G, et al. Hypoxia-induced pathological angiogenesis mediates tumor cell dissemination, invasion, and metastasis in a zebrafish tumor model. *Proceedings of the National Academy of Sciences of the United States of America*. 2009; 106:19485–90. [PubMed: 19887629]
25. Sharma SV, Lee DY, Li B, Quinlan MP, Takahashi F, Maheswaran S, et al. A chromatin-mediated reversible drug-tolerant state in cancer cell subpopulations. *Cell*. 2010; 141:69–80. [PubMed: 20371346]
26. Carlino MS, Gowrishankar K, Saunders CA, Pupo GM, Snoyman S, Zhang XD, et al. Antiproliferative effects of continued mitogen-activated protein kinase pathway inhibition following acquired resistance to BRAF and/or MEK inhibition in melanoma. *Molecular Cancer Therapeutics*. 2013; 12:1332–42. [PubMed: 23645591]
27. Haarberg HE, Paraiso KH, Wood E, Rebecca VW, Sondak VK, Koomen JM, et al. Inhibition of Wee1, AKT, and CDK4 underlies the efficacy of the HSP90 inhibitor XL888 in an in vivo model of NRAS-mutant melanoma. *Molecular cancer therapeutics*. 2013; 12:901–12. [PubMed: 23538902]
28. Udayakumar D, Zhang G, Ji Z, Njauw CN, Mroz P, Tsao H. EphA2 is a critical oncogene in melanoma. *Oncogene*. 2011; 30:4921–9. [PubMed: 21666714]
29. John JK, Paraiso KH, Rebecca VW, Cantini LP, Abel EV, Pagano N, et al. GSK3beta Inhibition Blocks Melanoma Cell/Host Interactions by Downregulating N-Cadherin Expression and Decreasing FAK Phosphorylation. *The Journal of investigative dermatology*. 2012; 132:2818–27. [PubMed: 22810307]

Significance

This study provides evidence that BRAF inhibition promotes the adoption of a reversible, therapy-driven metastatic phenotype in melanoma. The co-targeting of ligand-independent EphA2 signaling and BRAF may be one strategy to prevent the development of therapy-mediated disease at new sites.

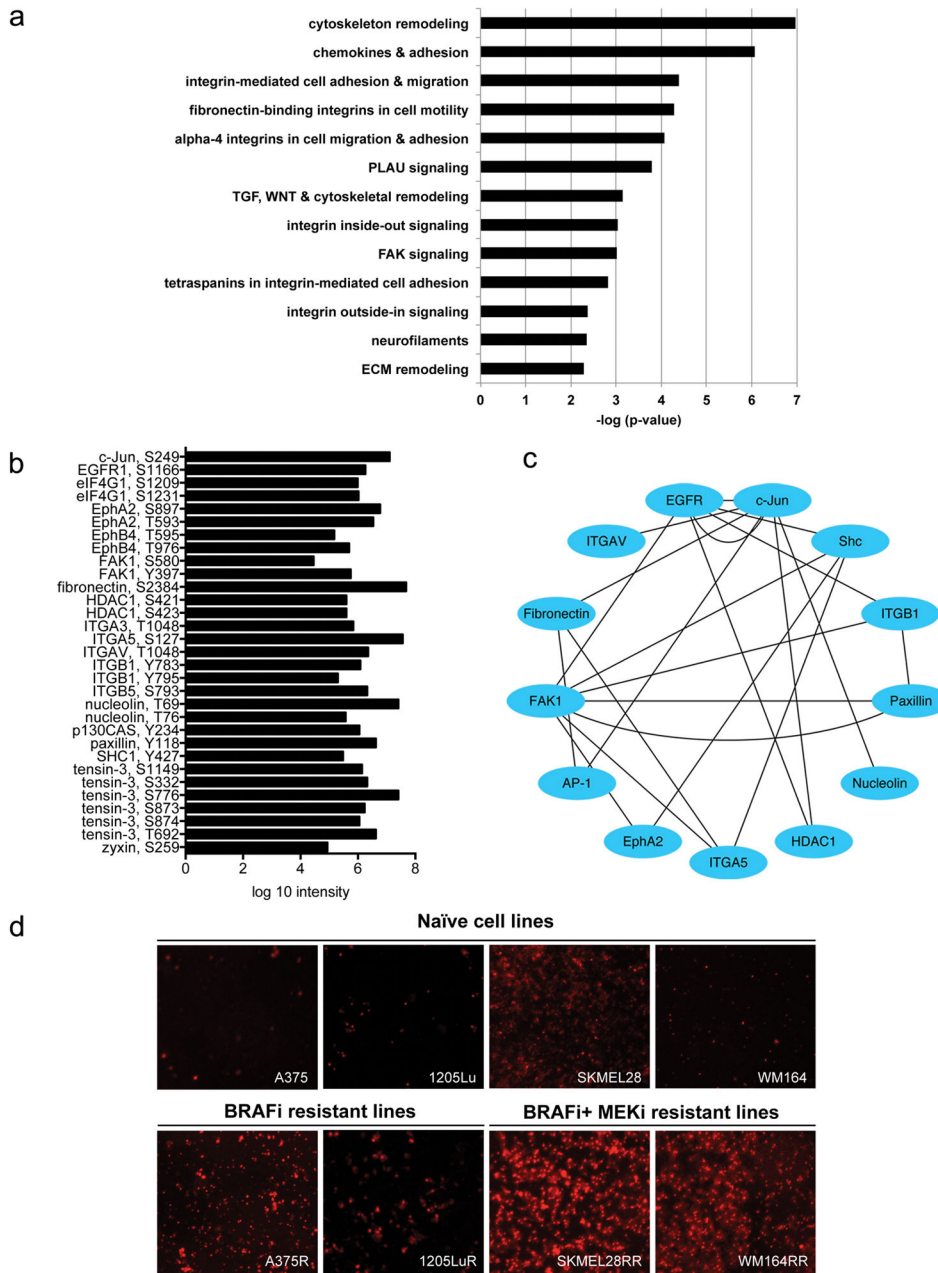


Figure 1. Comprehensive phosphoproteomics identifies an invasive, motile signaling signature associated with BRAF inhibitor resistance

A: GeneGo enrichment analysis revealed several highly significant pathways ($-\log p\text{-value} > 2$) appearing within the resistance interactome. **B:** Further enrichment analysis of the resistance network showed that several proteins were not only found to be increased (\log_{10} relative peak intensity) following acquired resistance but also recurred across several of the resistance pathways. **C:** As these proteins would broadly contribute to resistance we conducted a connectivity analysis that revealed that the redundant nodes formed a highly connected sub-network. **D:** Acquired resistance to MAPK inhibition leads to increased invasion and migration as seen by modified Boyden chamber assays. Human vascular

endothelial cells (HUVECs) were plated onto transwell inserts and grown to confluency. DiI labeled (red fluorescence) naïve or resistant melanoma cells were then plated on top of the HUVEC layer and allowed to invade. Non-migratory cells were removed and the remaining cells were imaged by fluorescence microscopy.

Author Manuscript

Author Manuscript

Author Manuscript

Author Manuscript

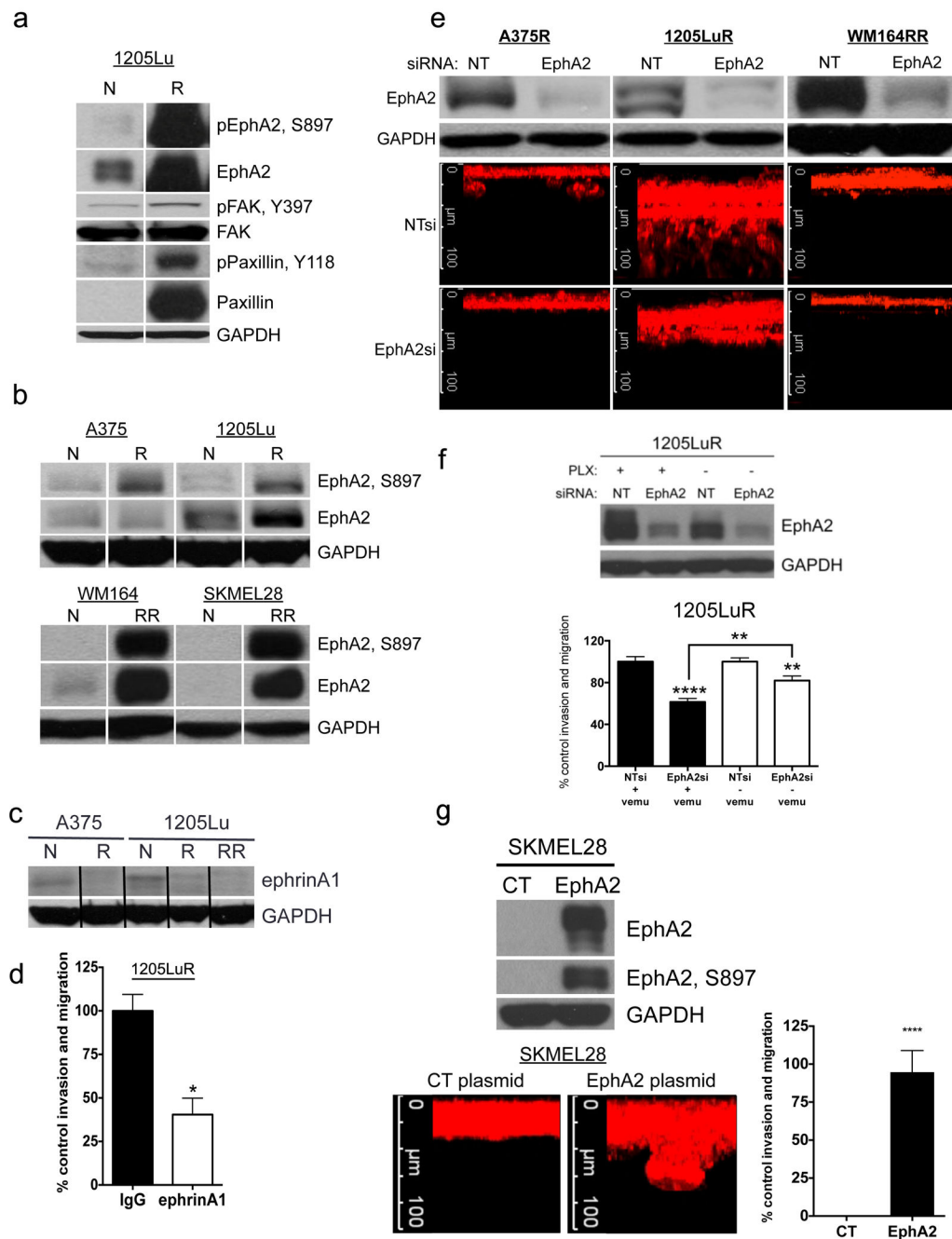


Figure 2. BRAF and BRAF/MEK inhibition induces an invasive phenotype driven through ligand-independent ephrin-A2 signaling

A: Western Blot validation of increased total EphA2, phospho-EphA2 (S897), phospho-FAK (Y397), phospho-Paxillin (Y118) and paxillin expression in BRAF inhibitor resistant (R) vs naïve (N) 1205Lu melanoma cells. **B:** Increased EphA2 and S897-EphA2 expression is observed in multiple models of BRAF (R) and BRAF/MEK (RR) inhibitor resistance. **C:** Ephrin-A1 ligand expression is decreased in cell lines with BRAF (R) and BRAF/MEK inhibitor (RR) resistance. **D:** Ephrin-A1 ligand prevents invasion of 1205LuR cells through matrigel. Cells were treated with Ephrin-A1 ligand (1 μ g/ml, 24 hrs) **E:** siRNA EphA2

reverses the invasive phenotype of BRAF (R) and BRAF/MEK (RR) resistant cell lines. siRNA knockdown of EphA2 and representative images of reduced matrigel invasion. **F:** Knockdown of EphA2 reduces invasion in the absence and presence of vemurafenib. Vemurafenib resistant 1205LuR cells were transfected with 25nM non-targeting siRNA (NTsi) or 25nM EphA2 siRNA in the absence of vemurafenib. After 24 hours, fresh media with 3 μ M vemurafenib (black bars) or DMSO (white bars) was added. **G:** Introduction of EphA2 enhances invasion of SK-MEL-28 cells into collagen. SK-MEL-28 cells were transfected with a plasmid containing EphA2 and selected for 14 days. After this time cells were plated on top of matrigel and allowed to invade. Image shows a Z-stack of phalloidin-stained melanoma cells through matrigel invading towards serum. Bar graph shows the quantification of invasion relative to control.

Author Manuscript

Author Manuscript

Author Manuscript

Author Manuscript

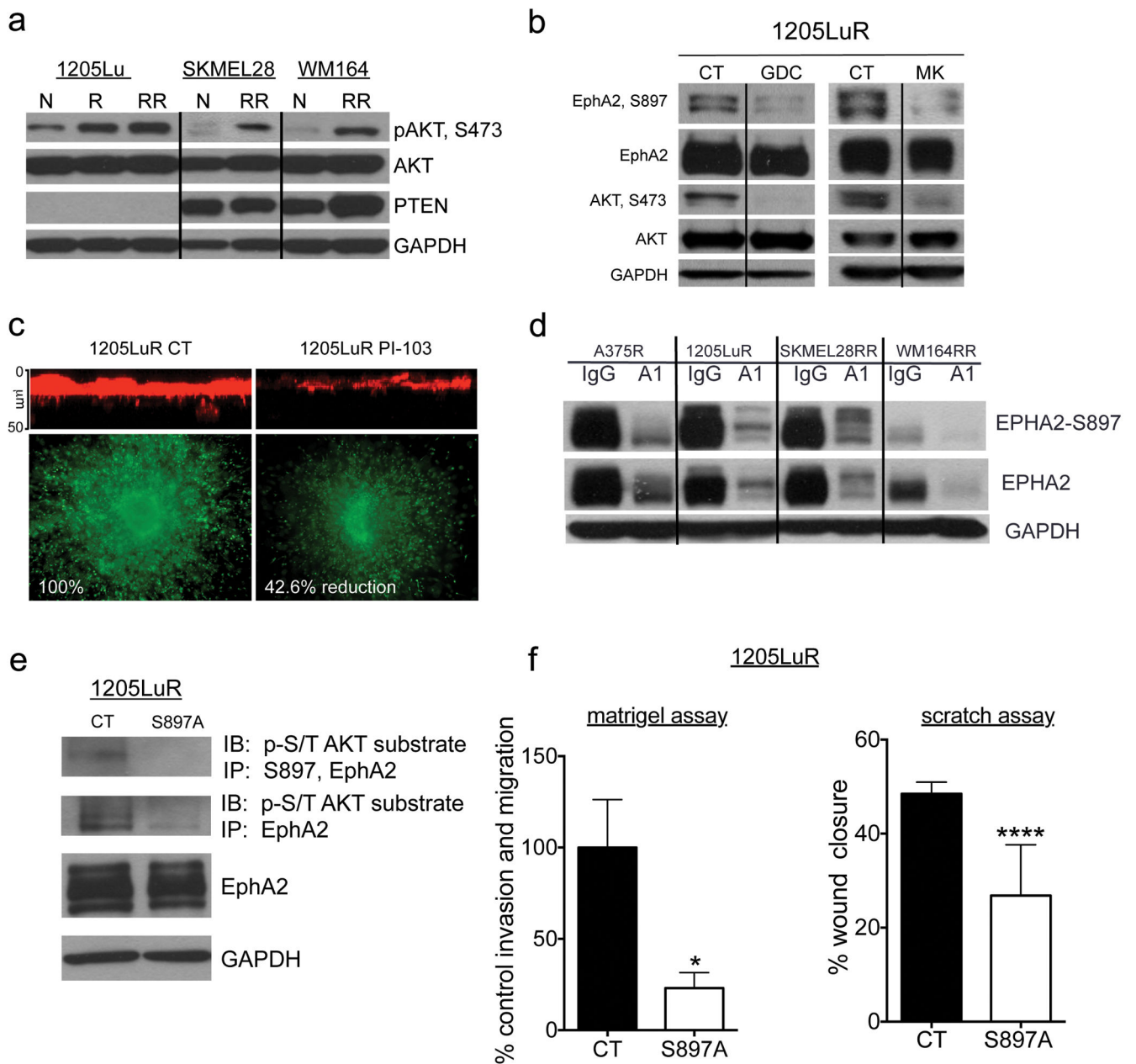


Figure 3. Ligand-independent phospho-EphA2 (S897) signaling is PI3K/AKT dependent

A: Western blot showing expression of pAKT, AKT, PTEN and GAPDH in melanoma cells that are drug naïve (N), BRAF inhibitor resistant (R) and BRAF/MEK inhibitor resistant (RR). **B:** The PI3K inhibitor GDC-0941 (3 μ M, 24 hr) or the AKT inhibitor MK-2206 (3 μ M, 1 hr) decreases the phosphorylation of AKT (S473) and EphA2 (S897). **C:** PI3K inhibition reduces the invasion of BRAF inhibitor resistant melanoma cell lines. (Top panel) 1205LuR cells were plated on top of Matrigel and treated with either vehicle or PI-103 (1 μ M) for 24 hrs before being stained with phalloidin and imaged using confocal microscopy. (Bottom panel) 1205LuR cells were grown as 3D spheroids, implanted into collagen and treated with vehicle or 1 μ M PI-103 prior to staining with calcein AM. Invading

cells were imaged with an inverted fluorescence microscope and levels of invasion were calculated with ImageJ software. **D:** Ephrin-A1 ligand reduces EphA2 (S897) phosphorylation levels in 1205LuR cells. Cells were treated with ephrin-A1 ligand (1 $\mu\text{g}/\text{mL}$, 24 hr) before being analyzed by Western Blot. **E:** Transfection of the EphA2 serine to alanine substitution at position 897 mutant plasmid (S897A) prevents S897 phosphorylation of EphA2. 1205LuR cells were transfected with either WT (control) or mutant S897A EphA2 plasmid. Lysates from transfected cells were immunoprecipitated with antibodies against S897 and total EphA2 and immunoblotted with anti-phospho-serine/threonine AKT substrate antibody. Total, non-immunoprecipitated protein was also probed for EphA2 and GAPDH as loading controls. **F:** Mutant S897A expression reduces 1205LuR cell invasion and scratch wound closure. 1205LuR cells transfected with WT (control) or S897A mutant EphA2 plasmid were either allowed to invade through matrigel or plated into 6 well tissue culture plates and grown to confluency before being scratched with a p20 pipet tip after which the wound was allowed to close over 24 hours.

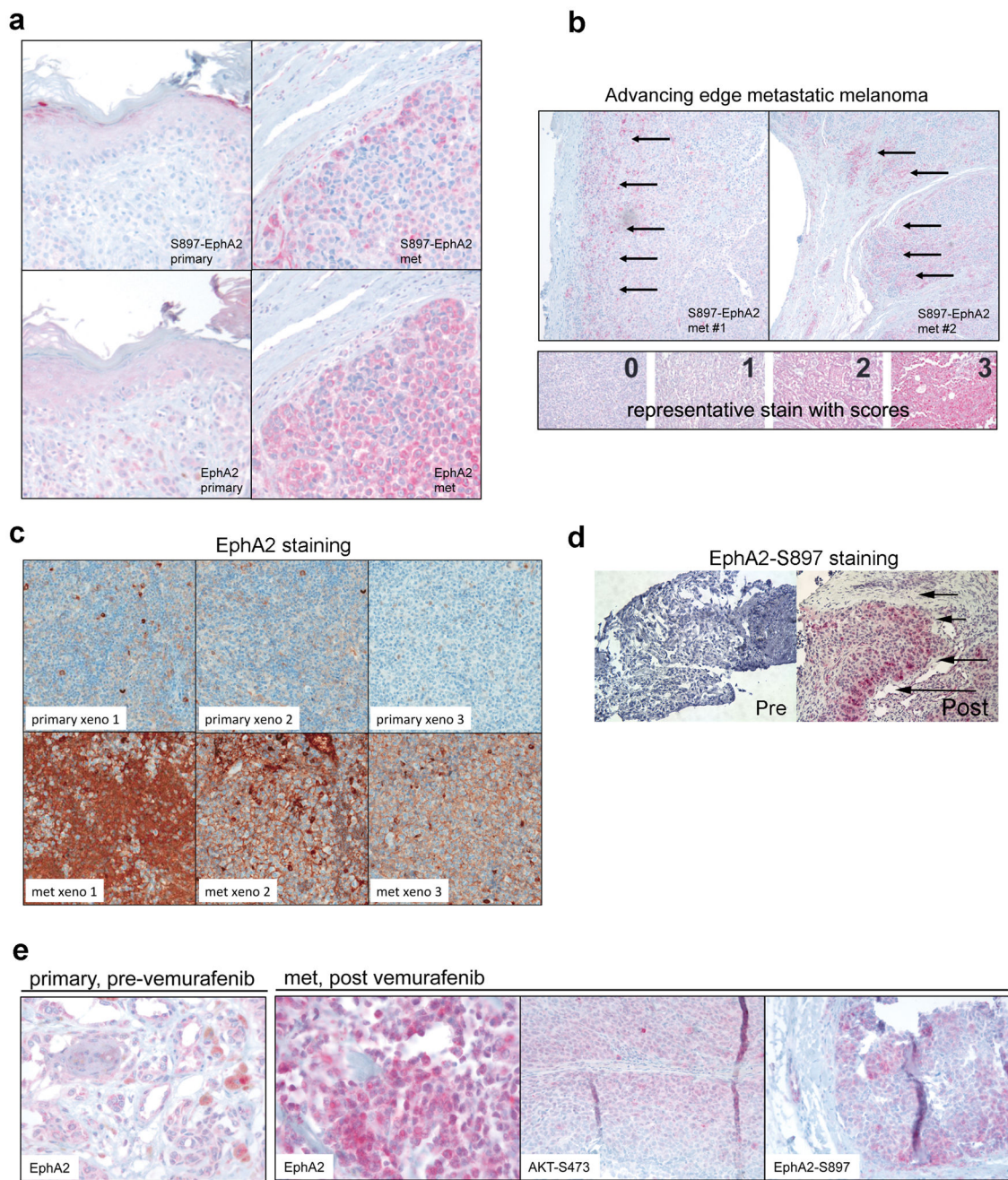


Figure 4. Increased total and phosphorylated (S897) EphA2 in clinical specimens is associated with metastatic dissemination

A: Representative images of sequentially sectioned primary (S897-EphA2: +1–2, total EphA2: +2) and metastatic (S897-EphA2: +2, total EphA2: +3) IHC stained patient tumor specimens. **B:** Metastasis is associated with higher tumor-wide positive staining (+2/3) for pEphA2, increased focal S897-EphA2 staining and greater tumor-wide total EphA2 staining. Representative images of pEphA2 staining of the advancing edge of 2 separate metastatic tumor specimens. Arrows indicate focal S897-EphA2 staining at the leading edge. **C:** Images from 3 matched pairs of primary and metastatic vemurafenib-treated patient derived

melanoma mouse xenografts stained for total EphA2 showing greatly increased levels of total EphA2 expression in the matched metastatic vs primary lesion. Images show paired samples from 3 independent mice. **D:** Vemurafenib treatment increases EphA2 expression in melanoma patient specimens. Representative images of staining for EphA2 and S897-EphA2 in matched melanoma lesions (from patient E) pre-treatment and collected on vemurafenib therapy. See Supplemental Table 2 for details. **E:** Vemurafenib resistance is associated with increased EphA2 expression in specimens derived from a patient with matched primary melanoma and metastatic lesions that emerged on therapy. Images show IHC staining for EphA2, S897 EphA2 and pAKT on a matched pair of primary (pre-vemurafenib treatment) and subcutaneous metastatic (post-vemurafenib treatment) lesions.

Author Manuscript

Author Manuscript

Author Manuscript

Author Manuscript